Clustering coefficient and periodic orbits in flow networks

Victor Rodríguez-Méndez,[1] Enrico Ser-Giacomi,[2] and Emilio Hernández-García[1]
[1)] *IFISC (CSIC-UIB), Instituto de Física Interdisciplinar y Sistemas Complejos, Campus Universitat de les Illes Balears, E-07122 Palma de Mallorca, Spain.*
[2)] *École Normale Supérieure, PSL Research University, CNRS, Inserm, Institut de Biologie de l'École Normale Supérieure (IBENS), F-75005 Paris, France*

(Dated: November 2, 2016)

We show that the clustering coefficient, a standard measure in network theory, when applied to flow networks, i.e. graph representations of fluid flows in which links between nodes represent fluid transport between spatial regions, identifies approximate locations of periodic trajectories in the flow system. This is true for steady flows and for periodic ones in which the time interval τ used to construct the network is the period of the flow or a multiple of it. In other situations the clustering coefficient still identifies cyclic motion between regions of the fluid. Besides the fluid context, these ideas apply equally well to general dynamical systems. By varying the value of τ used to construct the network, a kind of spectroscopy can be performed so that the observation of high values of mean clustering at a value of τ reveals the presence of periodic orbits of period 3τ which impact phase space significantly. These results are illustrated with examples of increasing complexity, namely a steady and a periodically perturbed model two-dimensional fluid flow, the three-dimensional Lorenz system, and the turbulent surface flow obtained from a numerical model of circulation in the Mediterranean sea.

arXiv:1609.03291v2 [nlin.CD] 10 Nov 2016

The Lagrangian description of fluid dynamics, which focuses on the motion of the fluid particles as they are advected by the flow, provides a useful bridge between the theory of dynamical systems and the analysis of fluid transport and mixing, so that techniques and results can be transferred from one field to the other. Modern network theory has also been brought into contact with fluid dynamics and dynamical systems through the concept of flow networks, in which the motion of fluid particles between different regions is represented by links in a graph. In this paper we use the flow network framework to show that the clustering coefficient, a standard measure in network theory, identifies periodic orbits, fundamental objects in the theory of dynamical systems and also of importance in the context of fluid motion.

I. INTRODUCTION

In the last years flow networks have been defined and analyzed to understand properties of fluid transport and mixing[1–4], with particular emphasis on geophysical transport and its biological implications[5–8]. The basis of the flow-network paradigm rests on addressing the Lagrangian fluid dynamics of the system with the so-called set-oriented methods[9–17] in which a discrete approximation to the motion of fluid is characterized by a transfer or Perron-Frobenius operator indicating which proportion of fluid is moved from one region to another by the flow. Under the name of 'mapping method' these ideas have provided insight on mixing and its optimization in the context of industrial flows[18–20]. Besides the context of fluid flows, the framework is also relevant to characterize the behavior of general dynamical systems[17,21–23]. The contact with network theory[24] is made when the matrix representing the transfer operator is interpreted as the adjacency matrix of a network[1–4,17,22,23], so that the weight of a link between two nodes is given by the amount of flow between the corresponding spatial locations. An alternative viewpoint in characterizing fluid flows with network techniques assigns links between spatial regions according to statistical correlations between their dynamical variables, leading to correlation-based flow networks[25–27] and making a connection with the broad field of climate networks[28–31].

Flow networks have been analyzed with standard measures of network topology, which have complemented the direct study with specific fluid dynamics methods. For example, degree and related properties of the different nodes have been related to local mixing and dispersion, with explicit correspondence with Lyapunov exponents and entropic measures[1]. Betweenness centrality highlights preferred transit nodes connecting distant regions[2]. Closeness and eigenvector centrality distinguish regions dominated by laminar or by strong mixing, and identify structures related to invariant manifolds[4]. Spectral and other community detection methods have been used to extract coherent regions and basins of attractions in the fluid flow[1,6,7,32–34].

There is however a standard network measure, the *clustering coefficient*, which has not yet been interpreted in the context of fluid flows. The aim of the present paper is to provide such interpretation. We show that, under some conditions, clustering characterizes in a useful way periodic trajectories in fluids and in dynamical systems, serving as a spectroscopic tool that detects the presence of periodic or close-to-periodic fluid paths of given period, and reveals their approximate location in space. Periodic orbits are objects of fundamental importance in the theory of dynamical systems[35] and in the context of fluid flow they identify recurrent fluid-element motions. Even when the conditions required to locate periodic trajecto-

ries are not perfectly fulfilled, the clustering coefficient still reveals interesting flow structures.

To achieve our aim we will consider examples representative of flows with an increasing level of complexity. After revising the methodology of network construction (Sect. II) and discussing the general relationship between clustering and closed paths in networks (Sect. III), we address in Subsect. IV A the simple situation of two-dimensional (2d) steady flows. In this case the associated flow network is also steady and the clustering measures have a clear meaning. The interpretation of these quantities are discussed for 2d periodic flows in Subsect. IV B and for a three-dimensional (3d) time-independent dynamical system in Subsect. IV C. A situation of fully aperiodic flow is briefly addressed in Subsect. IV D. The paper closes with a sections mentioning further extensions (Sect. V) and the Conclusions section (Sect. VI).

II. FLOW NETWORK CONSTRUCTION FROM FLUID MOTION

Fluid flow is a process occurring in continuous space. A network representation of it requires some kind of discretization or *coarse-graining*. We briefly remind here the basic steps needed to build discrete flow networks from the Lagrangian fluid dynamics[1,4].

First, the spatial domain occupied by the fluid is discretized in a large number N of boxes, $\{B_i, i = 1, ..., N\}$, so that network node j will represent the fluid box B_j. Although this is not strictly necessary, we take here for simplicity all boxes to have the same area or volume. Also, unless otherwise stated, we consider an incompressible flow of constant density. Then, all boxes contain the same amount of fluid.

To complete the definition of the transport network, we establish a directional *link* between two nodes when an exchange of fluid occurred between the corresponding fluid boxes during a given time interval. To do this, we use the fluid *flow map* $\Phi_{t_0}^{\tau}$:

$$\mathbf{x}(t_0 + \tau) = \Phi_{t_0}^{\tau}(\mathbf{x}_0) \tag{1}$$

which gives the position at time $t_0+\tau$ of the fluid particle started at $\mathbf{x}_0$ at time t_0, and that is obtained simply by integrating the equations of motion of the fluid elements in the velocity field $\dot{\mathbf{x}}(t) = \mathbf{v}(\mathbf{x}(t), t)$. By considering this Lagrangian motion of all fluid particles inside a region A we define the action of the fluid map on whole regions: $A(t_0+\tau) = \Phi_{t_0}^{\tau}(A(t_0))$. By applying the flow map to our discrete boxes, we obtain the amount of flow among each pair of nodes, which will be taken as the *weight* of the corresponding link. More explicitly, the fraction of the fluid that started at node i at time t_0 and ended up at node j after a time τ is given by[9–14]:

$$\mathbf{P}(t_0, \tau)_{ij} = \frac{m\left(B_i \cap \Phi_{t_0+\tau}^{-\tau}(B_j)\right)}{m(B_i)} \ . \tag{2}$$

The transfer or transport matrix $\mathbf{P}(t_0, \tau)_{ij}$ is a discrete approximation to the Perron-Frobenius operator of the flow. $m(A)$ is a measure assigned to the set A, which in our case is its area or volume (and, for constant density, the amount of fluid it contains). A probabilistic interpretation of Eq. (2) is that $\mathbf{P}(t_0, \tau)_{ij}$ is the probability for a particle to reach the box B_j, under the condition that it started from a uniformly random position within box B_i. We interpret $\mathbf{P}(t_0, \tau)$ as the adjacency matrix of a weighted and directed network, so that $\mathbf{P}(t_0, \tau)_{ij}$ is the weight of the link from node i to node j, for given t_0 and τ. $\mathbf{P}(t_0, \tau)$ is row-stochastic, i.e. it has non-negative elements and $\sum_{j=1}^{N} \mathbf{P}(t_0, \tau)_{ij} = 1$. For incompressible flows it is also doubly stochastic.

A standard numerical estimation of (2) is obtained by randomly placing at time t_0 a large number of particles N_i inside each box B_i (with our equal area/volume choice, all N_i should be equal), and determine with the flow map in which boxes are the final positions at time $t_0 + \tau$. Then:

$$\mathbf{P}(t_0, \tau)_{ij} \approx \frac{\text{number of particles from box } i \text{ to box } j}{N_i} \ . \tag{3}$$

Networks constructed from $\mathbf{P}(t_0, \tau)$ are *weighted* and *directed*[24]. In addition, the dependence on t_0 gives in fact a different network for each starting time t_0. We can consider the sequence $\{\mathbf{P}(t, \tau), t = t_0, t_1, ...\}$ as a *temporal* network[36], i.e. a network which is changing in time. The case in which $\mathbf{P}(t_0, \tau)$ is independent on the initial time t_0 gives a *static* network. This occurs when the flow velocity field is steady: $\mathbf{v}(\mathbf{x}, t) = \mathbf{v}(\mathbf{x})$.

It is standard[15,34,37] to make a Markovian approximation for the dynamics at times beyond τ: we assume that the transport matrix at long times is well approximated by a product of matrices at shorter times, $\mathbf{P}(t_0, n\tau) = \mathbf{P}(t_0, \tau)\mathbf{P}(t_0+\tau, \tau)...\mathbf{P}(t_0+(n-1)\tau, \tau)$. This amounts to assuming that at the beginning of each time interval the fluid particles are reinitialized with uniform density in each box, losing memory of their earlier positions. The assumption is equivalent to introducing some artificial diffusion in the dynamics[38]. In the limit of very small boxes and very short time steps, the approximation becomes correct[38], as this computational diffusion vanishes and we recover the exact Lagrangian dynamics given by (1). For finite boxes the added diffusion can be thought as modeling unresolved scales of motion.

A path in a network is an ordered set of nodes $\{i, j, k, ...\}$ such that there is a non-vanishing link between each consecutive pair of nodes. A *time-respecting path*[36] can be defined for a temporal network $\{\mathbf{P}(t, \tau), t = t_0, t_1, ...\}$ as a sequence of nodes $\{i, j, k, ...\}$ such that there is a non-vanishing link between i and j for the first time interval $[t_0, t_1]$, a non-vanishing link between j and k for the second interval $[t_1, t_2]$, etc. Time-respecting paths characterize transport in the flow network[2,3,39]. Since nodes are finite regions of flow, time-respecting paths can be though as 'tubes' of fluid trajectories giving a coarse-grained version of them. When no confusion could arise

we would refer to time-respecting paths also as *trajectories*. Of course, for static networks there is no distinction between paths and time-respecting paths.

Many properties of networks defined by the transport matrix $\mathbf{P}(t_0,\tau)$ have been already analyzed, as summarized in the Introduction. We now consider the clustering coefficient.

III. CLUSTERING COEFFICIENT AND CLOSED PATHS

The clustering coefficient of a node measures the amount of closed triangles in the network of which that node is a vertex.[40,41]. Depending on the type of network (weighted, directed, ...) and of the kind of triangles one is interested in, different clustering coefficients can be defined[42,43]. Triangles in a graph give closed paths and then it is natural to look for relationships between these triangles and closed trajectories of the fluid elements, the signature of periodic orbits of the associated advection dynamical system. An essential characteristic of the fluid trajectories is its directionality. Thus, considering the *directed* character of the flow network would be an important ingredient to take into account when defining a clustering coefficient of relevance in the study of fluid flows. To focus more clearly on this relevant aspect we will neglect in the following the weighted character of flow networks, by considering the unweighted network defined by the adjacency matrices $\mathbf{A}(t_0,\tau)$, binary versions of the transport matrices $\mathbf{P}(t_0,\tau)$:

$$\begin{aligned} &\mathbf{A}(t_0,\tau)_{ij}=1 \quad \text{if } \mathbf{P}(t_0,\tau)_{ij}>0 \text{ and } i\neq j \\ &\mathbf{A}(t_0,\tau)_{ij}=0 \quad \text{if } \mathbf{P}(t_0,\tau)_{ij}=0 \ \text{ or } i=j\ . \end{aligned} \tag{4}$$

$\mathbf{A}(t_0,\tau)$ still keeps the connectivity and directional information, as well as the time-evolving character through the time-dependence on t_0. Let us consider first the single network defined by $\mathbf{A}(t_0,\tau)$ for fixed t_0. Not all triangles present there are related to closed paths. Figure 1 shows four possible configurations of the directions in the edges of a triangle involving nodes A, B and C. Only configuration a), which is called a *cyclic* triangle[43], gives a triangle that can be related to a closed path $A\to B\to C\to A$. Given a node i with in-degree $k_i^{IN}=\sum_{j\neq i}\mathbf{A}_{ji}$, out-degree $k_i^{OUT}=\sum_{j\neq i}\mathbf{A}_{ij}$ and with k_i^B of these links being bidirectional ($k_i^B=\sum_{j\neq i}\mathbf{A}_{ij}\mathbf{A}_{ji}$), a *cyclic clustering coefficient* C_i^c is defined as the ratio of all cyclic triangles involving node i present in the network, divided by all possible cyclic triangles that could have been constructed with these values of k_i^{IN}, k_i^{OUT}, k_i^B. It can be computed[43] from the diagonal elements of the third power of the adjacency matrix $\mathbf{A}$:

$$C_i^c=\frac{\left(\mathbf{A}^3\right)_{ii}}{k_i^{IN}k_i^{OUT}-k_i^B}\ . \tag{5}$$

With the particular normalization in Eq. (5), $C_i^c\in[0,1]$. But, since we have already neglected weight information, we will not pay much attention to the particular value of C_i^c. Rather the interesting point is if it is zero or not. In the last case there is at least one directed triangle involving i in the network. What is the meaning of this when the network represents a fluid flow, with binary adjacency matrix $\mathbf{A}(t_0,\tau)$? It means that there are at least two intermediate nodes m, n such that during the time interval $[t_0,t_0+\tau]$, some fluid particles have been transported from i to m, some from m to n, and some from n to i. Note that then, the values of C_m^c and C_n^c are also non-zero.

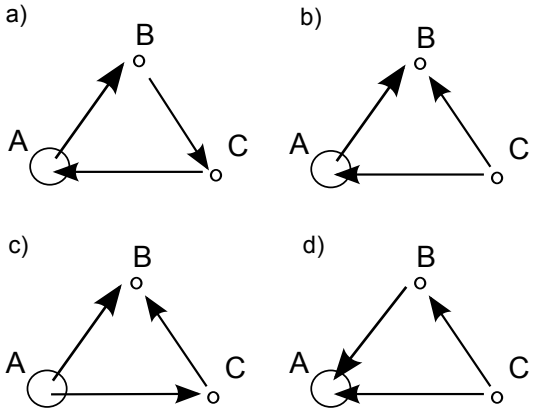

FIG. 1. Four distinct configurations of the directions of the edges in a triangle involving nodes A, B and C. Case a) is a cyclic triangle. Node A in configuration c) acts as a source, whereas it is a sink in configuration d). A is just an intermediate node in configuration b).

In the case of a steady flow, the flow network will be time-independent, and the dependence on the initial time t_0 in the transport and adjacency matrices will disappear: $\mathbf{P}(t_0,\tau)=\mathbf{P}(\tau)$, $\mathbf{A}(t_0,\tau)=\mathbf{A}(\tau)$. In this situation (under the Markovian assumption mentioned above), there will be fluid particles actually following the cycle $i\to m\to n$ during a time interval of duration 3τ. Nodes i with non-vanishing C_i^c will be part of time-respecting paths, i.e. coarse-grained fluid trajectories, of period 3τ. Since fluid trajectories are continuous and different points on them can be associated with different values of t_0, the invariance of $\mathbf{A}$ with respect to t_0 implies that the nodes with non-vanishing clustering will arrange in (thick) lines providing approximations to periodic orbits of period 3τ.

The situation is very similar if the flow is periodic with the same period τ as the duration of the time-interval used to construct the network (or a submultiple of it). In this case $\mathbf{P}(t_0+\tau,\tau)=\mathbf{P}(t_0,\tau)$ (the same is valid for $\mathbf{A}(t_0,\tau)$) and the repeated action at consecutive times of the transport process is given by powers of a single matrix $\mathbf{P}(t_0,\tau)$. At variance with the static case, the dependence on t_0 remains (and it is periodic). Nodes of high clustering will again give an approximation to the position at time t_0 of periodic orbits of period 3τ. In general these nodes will not form continuous lines, instead the nodes with high clustering will move following

the full trajectory by changing t_0.

If the integration time τ defining the flow network does not coincide with the period of the flow (or a multiple of it) the nodes with a high clustering coefficient are more difficult to interpret. It is still true that there is motion of fluid particles between nodes $i \to n \to m$ during the time interval $[t_0+\tau, \tau]$. But after this time the new transport matrix $\mathbf{P}(t_0+\tau, \tau)$ will be different from $\mathbf{P}(t_0, \tau)$ and then there is no guarantee that the same motion will repeat three times to produce a periodic time-respecting path of period 3τ. The situation is indeed similar to that of a fully aperiodic or turbulent flow, which keeps an arbitrary t_0 dependence on $\mathbf{P}(t_0, \tau)$ and $\mathbf{A}(t_0, \tau)$.

IV. APPLICATION TO SPECIFIC FLOWS

A. Steady two-dimensional flow

In this section and in the following we consider an analytic model flow, the *double-gyre*, which provides a convenient workbench to relate fluid dynamics quantities to network characteristics. See for example[44,45] for basic properties of this system and computations of its Lagrangian coherent structures and Lyapunov fields. Flow networks have already been constructed from it[3,4]. The double-gyre is a two-dimensional time-periodic flow defined in the rectangular region of the plane, $\mathbf{x} = (x, y) \in [0, 2] \times [0, 1]$. It is described by the streamfunction

$$\psi(x, y, t) = A \sin(\pi f(x, t)) \sin(\pi y) \ , \tag{6}$$

with

$$f(x, t) = a(t)x^2 + b(t)x \tag{7}$$

$$a(t) = \epsilon \sin(\omega t) \ , \tag{8}$$

$$b(t) = 1 - 2\epsilon \sin(\omega t) \ . \tag{9}$$

From these expressions, the velocity field is

$$\dot{x} = -\frac{\partial \psi}{\partial y} = -\pi A \sin(\pi f(x, t)) \cos(\pi y) \tag{10}$$

$$\dot{y} = \frac{\partial \psi}{\partial x} = \pi A \cos(\pi f(x, t)) \sin(\pi y) \frac{\partial f(x, t)}{\partial x} \ . \tag{11}$$

We take $A = 0.1$. We consider in this subsection $\epsilon = 0$, for which the flow is steady, $f(x, t) = x$, and the terms containing the periodic forcing are absent. This provides a simple test case to check the behavior of the clustering coefficient. Ideal fluid particles follow very simple trajectories: they rotate following closed streamlines, clockwise in the left half of the rectangle, and counterclockwise in the right one. The central streamline $x = 1$, a heteroclinic connection between the hyperbolic point at $(1, 1)$ and the one at $(1, 0)$, acts as a separatrix between the two regions. There are hyperbolic fixed points at $(x, y) = (0, 0), (1, 0), (2, 0), (0, 1), (1, 1), (1, 2)$ and elliptic fixed points at $(x, y) = (0.5, 0.5)$ and $(1.5, 0.5)$. The frequency of the orbits close to the elliptic points can be obtained by linearization, giving $\omega_0 = \pi^2 A$, from which the period is $T_0 = 2/(\pi A) \approx 6.366$. The orbits arrange concentrically around each elliptic point, with period increasing from T_0 when increasing the distance to the elliptic point and diverging for the nearly-square orbits that are close to touch the domain walls and the central $x = 1$ separatrix.

We discretize the fluid domain into $100 \times 50 = 5000$ square boxes, so defining the nodes in our flow network (each node thus represents a square region of size 0.02×0.02). The transport matrix $\mathbf{P}(t_0, \tau) = \mathbf{P}(\tau)$ is computed by releasing 400 particles from each of the boxes. We analyze the resulting clustering of each node for different values of τ.

Figure 2 clearly shows how the clustering coefficient computed from a flow network of interval τ highlights the periodic orbits of period close to 3τ: For small τ (not shown) clustering is essentially zero everywhere. When $\tau = 2$ clustering begins to be nonzero for nodes close to the origin, revealing the presence there of periodic orbits of period approximately $3 \times 2 = 6$. The exact linear period close to the origin is $T_0 = 6.366$, increasing outwards. This kind of 'resonance' at $3\tau = 6$ is broad, revealing the orbits for τ somehow larger and smaller than the one corresponding to the exact value $T_0/3 = 2.122$. When increasing τ, orbits further from the origin are highlighted, corresponding to the larger period. For τ sufficiently large, orbits with period submultiple of 3τ are also detected (the origin again for $\tau \approx 4$, a second orbit with period close to 7.5 for $\tau = 5$, etc.)

B. Periodic two-dimensional flow

We consider now the periodically forced double gyre, i.e. Eqs. (6)-(11) with $\epsilon > 0$. The remaining parameters are the same as in the previous subsection with the addition of the forcing frequency, which we take to be $\omega = 2\pi/5$ so that the flow period is $T = 5$, and the initial time that we always take as $t_0 = 0$. The procedure of discretization and particle releasing needed to define the flow network are also the same as in the previous Subsect. IV A. When $\epsilon > 0$, complex behavior including chaotic trajectories arises. The periodic perturbation breaks the central separatrix and now some interchange of fluid is possible between the left and the right parts of the domain. The geometric structures involved in this interchange have been studied with a variety of techniques[44,45].

The cleanest interpretation of the clustering coefficient is obtained when the flow network is computed during one period of the forcing, i.e. for $\tau = T = 5$, so that $\mathbf{P}(t_0+\tau, \tau) = \mathbf{P}(t_0, \tau)$ and a single matrix (and thus a single network) describes the full dynamics. In this case clustering is expected to be high in the regions surrounding the locations of the orbits of period $3\tau = 3T$, i.e. the period-3 orbits. Submultiples of this period will also lead to non-vanishing clustering, which includes the case

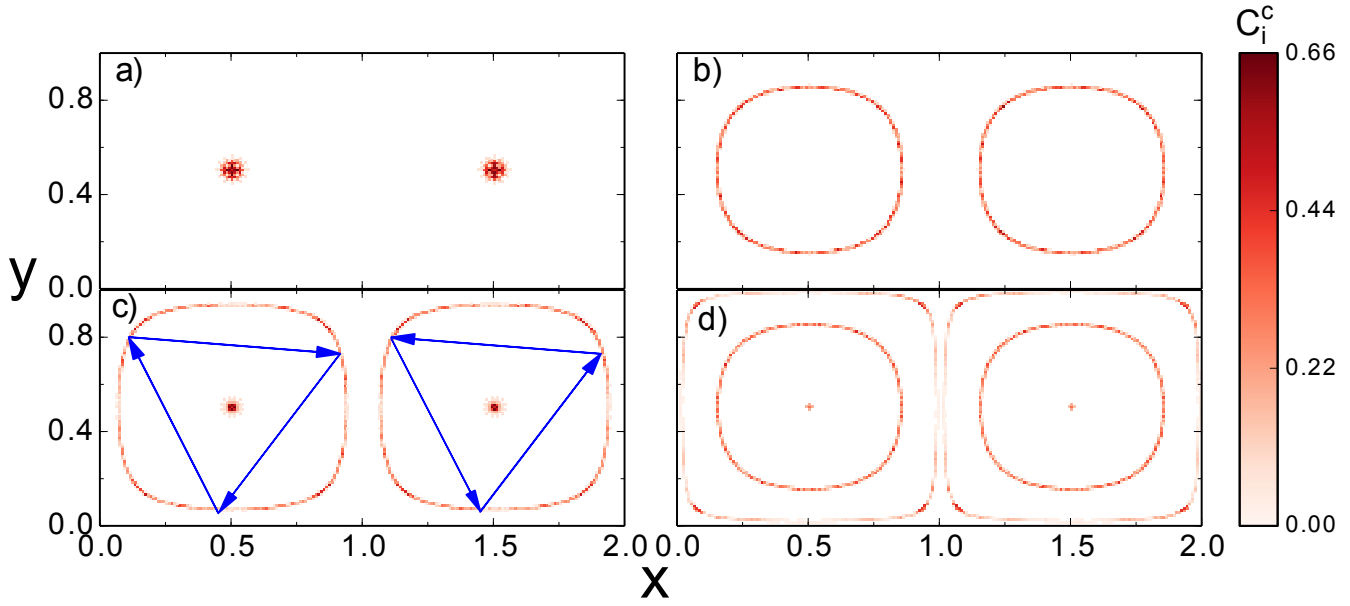

FIG. 2. Clustering coefficient C_i^c in the nodes of the flow network constructed from the steady ($\epsilon = 0$) double gyre flow with $A = 0.1$. a) $\tau = 2$, b) $\tau = 3$, c) $\tau = 4$, d) $\tau = 5$. Panel c) also shows two examples of cyclic triangles present in the system.

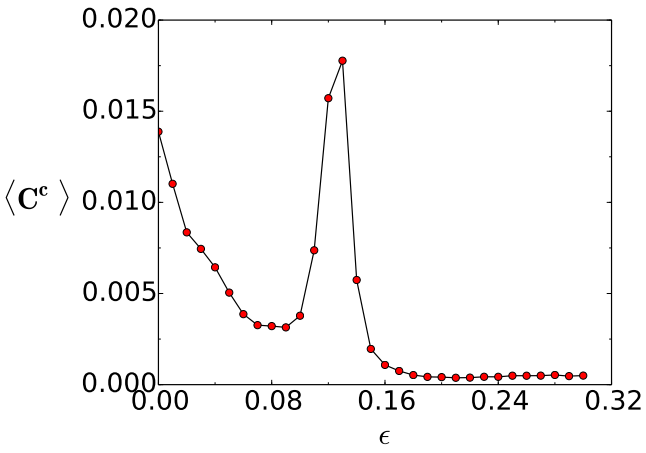

FIG. 3. Mean clustering coefficient per node $\langle C^c \rangle$ as a function of forcing intensity ϵ for the flow network with $A = 0.1$, $t_0 = 0$ and $\tau = 5$ equal to the flow period $2\pi/\omega$.

of period-1 orbits. The exact period-1 cycle is indeed excluded, because self-loops into a node are eliminated by the definition of the adjacency matrix $\mathbf{A}(t_0, \tau)$ in Eq. (4), but still we expect the tube of trajectories surrounding the periodic one, arising from the coarse-grained nature of the network description, to contain paths that connect to neighboring nodes and return some mass to the original one after three iterations, giving non-vanishing clustering.

In order to monitor the changes in the clustering spatial distributions as parameters are varied, we compute a global quantity, $\langle C^c \rangle$, the mean clustering per node. We display it in Fig. 3 as a function of ϵ. We see a marked peak occurring close to $\epsilon \approx 0.13$. Figure 4 shows the clustering coefficient of the different nodes in the network (panel a)) for $\epsilon = 0.12$, a value close to the maximum of $\langle C^c \rangle$, and compares it with the Poincaré section (panel b)) of the same flow at the same time $t_0 = 0$. We see that the dominant features in both the Poincaré representation and the clustering spatial distribution are the locations at $t_0 = 0$ of two period-1 orbits, each one surrounded by the three elements of an elliptic period-3 orbit (separated by the elements of the corresponding hyperbolic orbits of period-3, which have also non-zero C_i^c). For other parameters of the forcing these orbits are also present, as shown in Fig. 4c and d. Its footprint in the coarse-grained phase space defined by the network is however weaker as indicated by the smaller mean $\langle C^c \rangle$ in Fig. 3.

When the period of the flow does not coincide with the period τ used to define the network we are in a quasiperiodic situation that we expect to be similar to the case of aperiodic flows: we do not expect exact periodic orbits to be present. Nevertheless, we can still explore the behavior of the clustering with changing τ. Again transport of particles between regions A, B, C following the pattern $A \to B \to C \to A$ during the time interval $[t_0, t_0 + \tau]$ will lead to non-vanishing clustering, although we can not be sure that they will give periodic time-respecting paths after three iterations since flow will not be the same in the next intervals $[t_0 + n\tau, t_0 + (n+1)\tau]$. They will be approximate periodic paths if the flow changes slowly on the time scale τ. Figure 5 shows the mean clustering for fixed $\epsilon = 0.12$ and changing τ. There is a sharp peak at $\tau = 5$, as expected, since as shown before there are

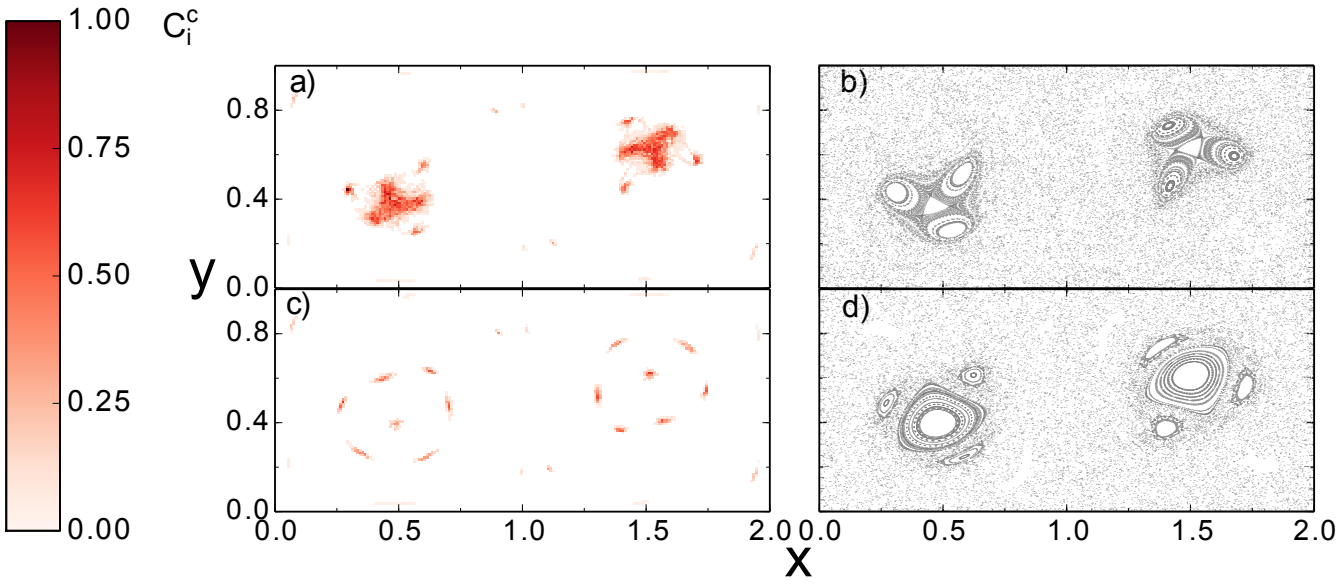

FIG. 4. Clustering coefficient (panels a) and c)) and Poincaré section at $t_0 = 0$ (panels b) and d)) for the flow network constructed from the double gyre with $A = 0.1$ and $2\pi/\omega = \tau = 5$. Panels a) and b): $\epsilon = 0.12$. Panels c) and d): $\epsilon = 0.09$.

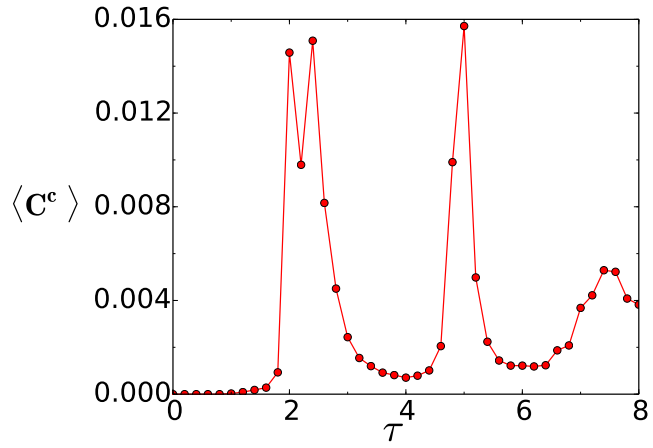

FIG. 5. Mean clustering coefficient per node $\langle C^c \rangle$ as a function of τ for the flow networks obtained from the double gyre with $A = 0.1$, forced periodically with $2\pi/\omega = 5$, $t_0 = 0$ and $\epsilon = 0.12$.

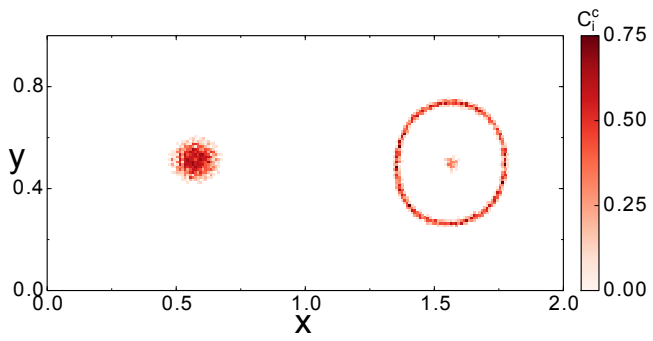

FIG. 6. Clustering coefficient of the nodes in the flow network of the double gyre with the parameters of Fig. 5 and $\tau = 2.2$.

cycles $A \to B \to C \to A$ which indeed lead to periodic trajectories. But we see also high values of clustering for $2 \lesssim \tau \lesssim 2.6$ indicating that cyclic triangles also occur during the interval $[t_0, t_0 + \tau]$ for these values of τ. Figure 6 shows that, certainly, these regions containing triangles are well visible in the system for $\tau = 2.2$. Their locations indicate that they are remnants of the $\epsilon = 0$ periodic orbits. They are no longer periodic, but between $[t_0, t_0 + \tau]$ with $t_0 = 0$ there is cyclic interchange of particles between these nodes.

C. Steady three-dimensional flow

For steady three-dimensional flows (and in general for steady d-dimensional flows), triangles $A \to B \to C \to A$ identified during an interval $[t_0, t_0 + \tau]$ will remain as triangles in successive intervals thus leading to periodic orbits of period 3τ. This is similar to the previously studied case of steady 2d flow but, at variance with it, here the periodic orbits are generically isolated and they could coexist in phase space with more complex chaotic trajectories. In order to explore a situation markedly distinct from the 2d steady double-gyre considered in Sect. IV A, which is an incompressible flow, here we consider a well known dissipative dynamical system, the Lorenz flow[46,47]. The trajectories $\mathbf{x}(t) = (x(t), y(t), z(t))$ are the

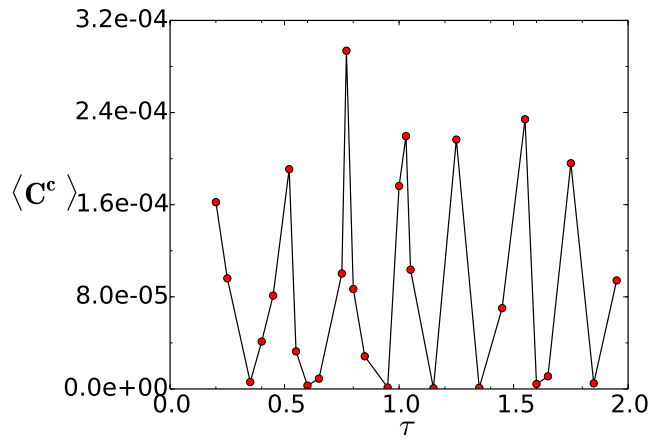

FIG. 7. Mean clustering coefficient per node $\langle C^c \rangle$ as a function of τ for the Lorenz system.

solutions of the system of equations:

$$\begin{aligned} \dot{x} &= s(y-x) \\ \dot{y} &= rx - y - xz \\ \dot{z} &= -bz + xy \ . \end{aligned} \tag{12}$$

We discretize the $(x, y, z) \in [-20, 20] \times [30, 30] \times [0, 50]$ portion of phase space into 31616 cubic boxes, so defining the nodes in our flow network (each node thus represents a cubic region of lateral size approximately 1.59 units). The transport matrix $\mathbf{P}(t_0, \tau)$ is computed by releasing 1000 particles from each of the boxes. We take the well studied parameter set $s = 10$, $b = 8/3$, $r = 28$ for which the chaotic Lorenz attractor is well developed and dominates the dynamics. In our initial condition all boxes have the same density, but under evolution the particles concentrate in the Lorenz attractor, leaving the rest of phase space empty. The presence of cyclic triangles is then expected only in the neighborhood of the attractor. Embedded in it there is an infinity of (unstable) periodic orbits of different periods[47,48]. These orbits have been computed by a variety of techniques[47–49] and are expected to give rise to non-vanishing clustering for the flow network of τ given by one third of the corresponding period. Figure 7 shows the mean clustering per node for the networks constructed from the Lorenz system at different values of τ. This provides a kind of 'spectroscopy' by which the presence of orbits of different periods is revealed. We see peaks at $\tau_1 = 0.52$, $\tau_2 = 0.77$, $\tau_3 = 1.03$, etc. which correspond very well (within the step sizes we have used to explore τ) to one-third of the period of the shortest periodic orbits of the system for these parameter values[48,49]: $3\tau_1 = 1.56$ resonates with the periodic orbit LR (meaning one turn to the left region of the Lorenz attractor and another turn right, repeated periodically) of period $T_1 \approx 1.5587$. The resonance at $3\tau_2 = 2.31$ reveals the LLR and RRL orbits, both with period $T_2 \approx 2.3059$. Next resonance, at $3\tau_3 = 3.09$ locates the presence of the orbits LLLR and RRRL, with $T_3 \approx 3.0236$, and LLRR, with $T_4 \approx 3.0843$ (our scan in τ and the node discretization has not been fine enough to distinguish between them).

To show that certainly the peaks in Fig. 7 correspond to 'resonances' of the value of τ with these periodic orbits of period 3τ we show in Fig. 8 the clustering coefficient of the different nodes together with the periodic orbits present at these values of τ. It is seen how the clustering coefficient identifies in a coarse-grained way the location of the periodic orbits.

D. Aperiodic flow

To explore the behavior of clustering in an aperiodic flow we use a surface velocity field obtained from the Mediterranean Forecasting System (MFS), an hydrodynamic model based on NEMO-OPA (Nucleus for European Modelling of the Ocean-PArallelis[50], version 3.2) at $1/16°$ horizontal resolution and 72 unevenly spaced vertical levels[51]. We consider the horizontal motion on the third layer below the surface corresponding to about 10 meters depth, which gives a good description of surface transport not excessively affected by wind stress.

The flow network is constructed[1,2,7] by discretizing the continuous ocean into quasi-square boxes of $1/8°$ horizontal size using an area-preserving sinusoidal projection. Each node is filled at t_0 with 100 ideal fluid particles, and their trajectories integrated during a time τ to get $\mathbf{P}(t_0, \tau)$.

Figure 9 shows a very broad 'resonance' for $3 \leq \tau \leq 16$ days which identifies potential cyclic motions of periods $9 - 48$ days, the range characteristic of energetic mesoscale structures such as eddies. Figure 10 displays the spatial distribution of the clustering coefficient for $\tau = 6$ days. The structures and their locations are reminiscent of ocean eddies, specially the ones that are semipermanent[52], such as the Alboran gyre (just east of Gibraltar strait), the Ionian anticyclones (east of Sicily) or the Shikmona gyre (south of Cyprus). Note that several of these objects have a concentric structure reminiscent of the nested periodic orbits of Fig. 2c,d or 6. For larger τ the structures become much weaker (smaller C_i^c) but also larger, suggestive of the big regional gyres in the Adriatic, the Tyrrhenian , etc. We do not expect perfect periodic orbits to be present in the turbulent particle motion produced by this ocean velocity field, but the small and slow displacements of the semipermanent gyres[52] detected by the clustering coefficient (Fig. 10) makes very likely that they contain nearly-periodic circulations with approximate period in a range including $3\tau = 18$ days. In fact, these structures have[52] radii of about 60-150 km and typical circulations speeds of 0.2-0.6 m/s , leading to circulation times in the range 7-40 days, consistent with the periods associated to the broad maximum of Fig. 9. In any case non-vanishing clustering reveals cyclic motions in the interval $[t_0, t_0 + \tau]$.

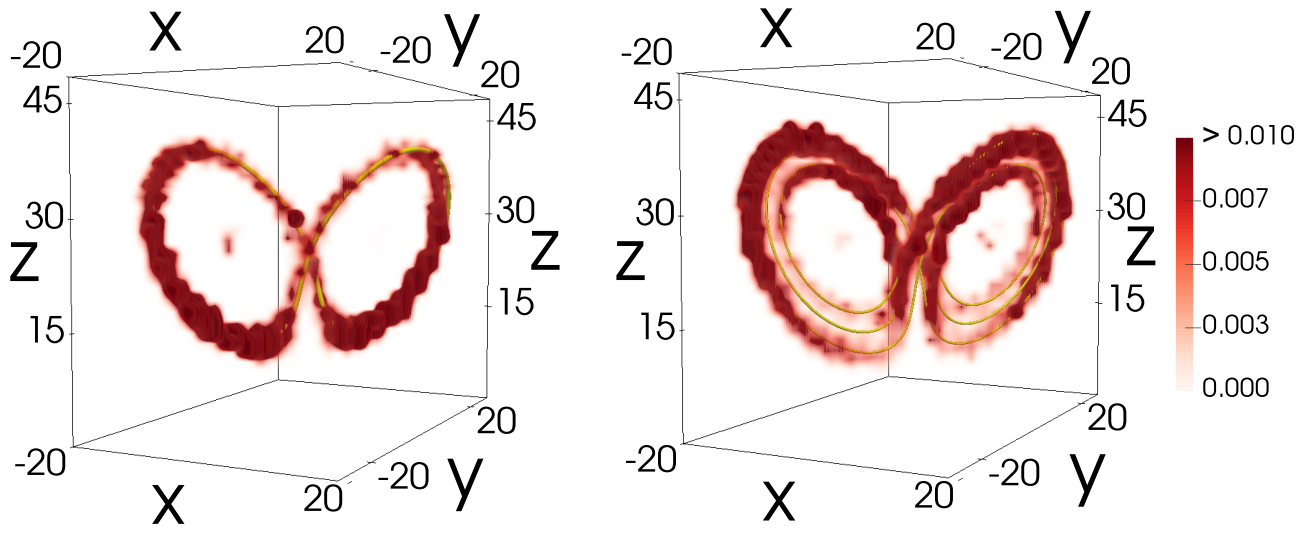

FIG. 8. Clustering coefficient for the flow network constructed for the Lorenz model at $\tau = 0.52$ (left) and $\tau = 0.77$ (right). Also plotted (yellow thick lines partially visible inside the red regions) are the periodic orbit LR (left) and the two periodic orbits LLR and RRL (right). To make visible all locations with nonvanishing C_i^c, nodes with clustering coefficient larger than the maximum indicated in the color bar are plotted with the same color.

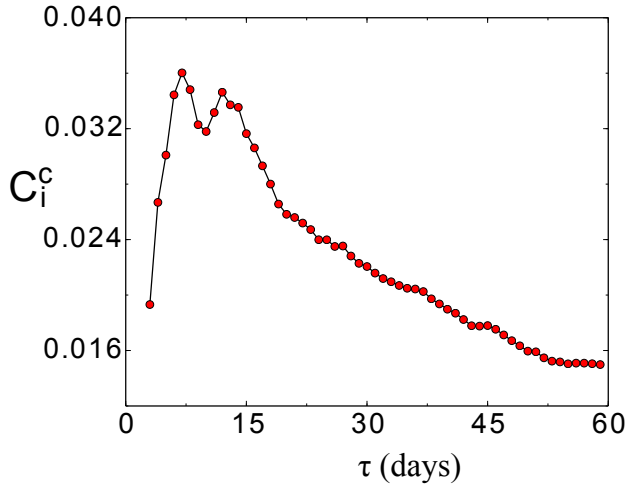

FIG. 9. Mean clustering coefficient per node $\langle C^c \rangle$ as a function of τ for the flow networks constructed from the MFS surface velocity field in the Mediterranean starting at $t_0 =$ January 1st 2010.

V. FURTHER EXTENSIONS

Standard clustering coefficients count triangles. But one can also count the number of rectangles, pentagons, etc. adjacent to a given node in a network. We have checked explicitly in the double-gyre flow example that, as expected, the generalized cluster coefficients highlight orbits of period 4τ, 5τ, etc. An example of this is shown in Fig. 11 for the double-gyre flow. We display a generalized clustering coefficient C_4 which is the number of cyclic polygons of 4 sides passing through each node. Panel a), constructed with $\tau = 3$ for the steady case, highlights the same orbit of period $4\tau = 12$ as in Fig. 2c. Panel b) displays C_4 for $\epsilon = 0.07$ and flow period $2\pi/\omega$ equal to the integration time $\tau = 5$. The locations of the central period-1 orbits are identified, as well as four spots around each of them corresponding to the two elements of elliptic and of hyperbolic period-2 orbits. There are however other features of difficult interpretation, apparently associated to the boundaries and to the central vertical separatrix. Also the central period-1 orbit is not apparent in Fig. 11a). We conclude that the generalized clustering coefficients contain in principle similar information to the standard triangular clustering, but in a more imprecise way arising probably from the extension of the Markov approximation to longer cycles.

An alternative characterization of triangular flow patterns which does not take into account the directional nature of flow can be done with the *undirected* cluster coefficient[41,43]. It is defined by constructing a new *undirected* network with adjacency matrix $\mathbf{U}$ such that $\mathbf{U}_{ij} = 1$ if either $\mathbf{A}_{ij} = 1$ or $\mathbf{A}_{ji} = 1$, and else $\mathbf{U}_{ij} = 0$. The degree of site i is now $k_i = \sum_{i \neq j} \mathbf{U}_{ij}$. The undirected clustering coefficient C_i^u is[41,43] the number of triangles in this new network involving site i, over the total number of possible triangles at that node for such degree $(k_i(k_i-1)/2)$:

$$C_i^u = \frac{\left(\mathbf{U}^3\right)_{ii}}{k_i(k_i-1)} \ . \tag{13}$$

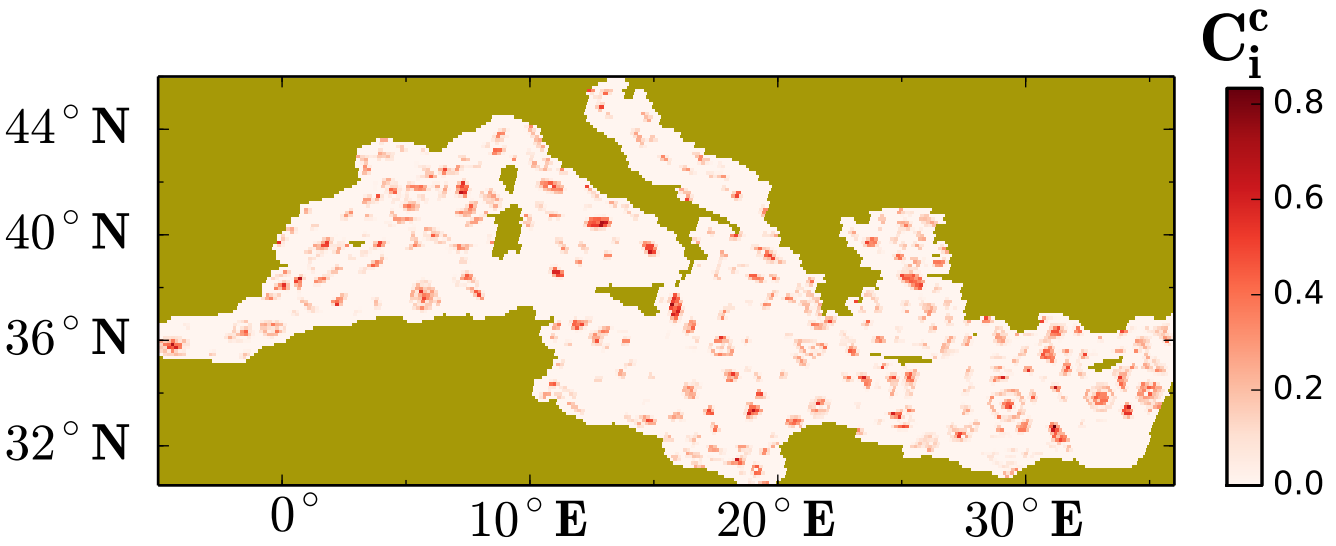

FIG. 10. Clustering coefficient of the nodes of the flow network constructed from the MFS surface velocity field in the Mediterranean with starting date January 1st 2010 and $\tau = 6$ days.

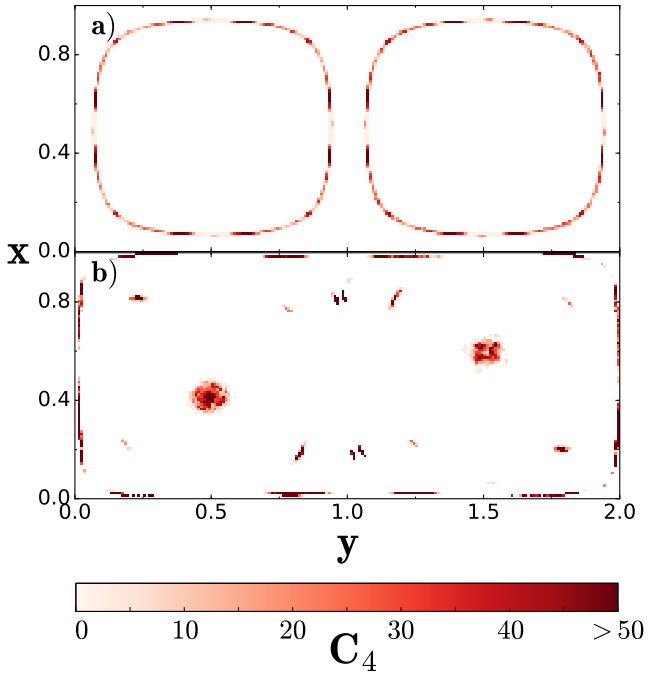

FIG. 11. Generalized clustering coefficient, C_4, counting the number of cyclic polygons of 4 sides at each node, for the double-gyre flow. a) Steady case, $\epsilon = 0$, $\tau = 3$; an orbit with period $4\tau = 12$ is highlighted. b) Periodic case with $\epsilon = 0.07$ and forcing period $2\pi/\omega = 5 = \tau$.

We have computed C_i^u for several of the flow examples considered above. For the double gyre case non-vanishing C_i^u occurs essentially in the same nodes as non-vanishing C_i^c. This indicates that nearly all triangles present in double-gyre flow networks are of the cycle type (type a) in Fig. 1). This may be due to the strong constraints imposed by the incompressibility of the flow. The situation for the Lorenz system, however, is completely different: the higher values of C_i^u occur in wide tubes that intersect the Lorenz attractor transversally, and that seem to trace portions of the stable manifolds of the non-vanishing unstable fixed points embedded in the attractor. We interpret this preliminary observation as revealing an abundance of triangles of type c) in Fig. 1: different particles released in node A, on a region close to the stable manifold of one of the fixed points, fall onto the attractor after a time τ at slightly different places, B and C, which are connected by the dynamics in the attractor. Further work is needed to establish if this observation is a general feature of dissipative dynamical systems or compressible flows, so that different clustering coefficients of the associated flow network would be useful to locate complex structures beyond periodic orbits.

We finally mention as another future development the full consideration of the weighted nature of the flow network, i.e. using matrix $\mathbf{P}$ instead of $\mathbf{A}$. We expect, for example, that triangle strength would be higher around stable trajectories as compared to unstable trajectories, since more fluid particles will remain close to the stable ones.

VI. CONCLUSIONS

In summary, for flow networks with integration time τ constructed for steady flows or for periodic ones of period τ (or submultiple of it), the cyclic clustering coefficient is non-vanishing in regions locating periodic orbits of pe-

riod 3τ. Both stable and unstable orbits are detected. Computation of the transport or adjacency matrices on which the network approach is based could be expensive (but easily parallelizable) because of the large number of Lagrangian particles that should be released. But once obtained, the matrices can be used to obtain a variety of flow diagnostics (Lyapunov exponents, community detection, and other applications mentioned in the Introduction). The computation of the clustering itself represents just a small computational overhead that gives access to an important aspect, periodicities, of flow transport.

Scanning a range of τ provides a kind of spectroscopic tool that gives high mean clustering per node at τ when periodic orbits of period 3τ exist and have large impact on the phase space of the system. Even for aperiodic networks clustering still identifies cyclic triangular paths during the interval $[0, \tau]$. They could again be interpreted as periodic trajectories in an approximate way when the time scale of change of the temporal network is slow compared to τ. It is likely that a more precise identification of periodic paths in aperiodic networks could be achieved by replacing the cyclic clustering coefficient by a *temporal* version of it, for example by replacing the third power of the single matrix $\mathbf{A}$ in Eq. (5) by a product of three adjacency matrices at consecutive times. This line of work is worth to be explored in the future.

At variance with standard methods to compute periodic trajectories in dynamical systems[53], clustering in networks highlights fluid nodes, which are finite regions, and then it detects thick tubes of trajectories instead of single pathways. Thus, this network approach can not compete with standard dynamical systems methods when *precision* in the location of periodic trajectories is required. Nevertheless the coarse-graining implied by the network discretization and the Markov approximation is equivalent to perturbing trajectories with diffusing noise[38] and thus our thick network paths would be very relevant objects when dealing with transport and dispersion in the presence of diffusion and/or noise. More in general, we expect that the connections among dynamical systems and network theory here proposed would open additional theoretical developments and fruitful transfer of concepts and methods across these two fields.

ACKNOWLEDGMENTS

We acknowledge financial support from Spanish Ministerio de Economía y Competitividad and Fondo Europeo de Desarrollo Regional under grants LAOP, CTM2015-66407-P (MINECO/FEDER) and ESOTECOS projects FIS2015-63628-C2-1-R (MINECO/FEDER), FIS2015-63628-C2-2-R (MINECO/FEDER). E.S-G. acknowledges partial support from the program "Investissements d'Avenir" launched by the French Government and implemented by ANR under grants ANR-10-LABX-54 MEMOLIFE and ANR-11-IDEX-0001-02 PSL* Research University.

[1] E. Ser-Giacomi, V. Rossi, C. López, and E. Hernández-García, "Flow networks: A characterization of geophysical fluid transport," Chaos **25**, 036404 (2015).
[2] E. Ser-Giacomi, R. Vasile, E. Hernández-García, and C. López, "Most probable paths in temporal weighted networks: An application to ocean transport," Physical Review E **92**, 012818 (2014).
[3] E. Ser-Giacomi, R. Vasile, I. Recuerda, E. Hernández-García, and C. López, "Dominant transport pathways in an atmospheric blocking event," Chaos **25**, 087413 (2015), 10.1063/1.4928704.
[4] M. Lindner and R. Donner, "Spatio-temporal organization of dynamics in a two-dimensional periodically driven vortex flow: a Lagrangian flow network perspective," Chaos **this issue, to appear** (2017).
[5] E. Treml, P. Halpin, D. Urban, and L. Pratson, "Modeling population connectivity by ocean currents, a graph-theoretic approach for marine conservation," Landscape Ecol. **23**, 19–36 (2008).
[6] M. N. Jacobi, C. André, K. Döös, and P. R. Jonsson, "Identification of subpopulations from connectivity matrices," Ecography **35**, 1004–1016 (2012).
[7] V. Rossi, E. Ser-Giacomi, C. López, and E. Hernández-García, "Hydrodynamic provinces and oceanic connectivity from a transport network help designing marine reserves," Geophysical Research Letters **41**, 2883–2891 (2014).
[8] M. Dubois, V. Rossi, E. Ser-Giacomi, S. Arnaud-Haond, C. López, and E. Hernández-García, "Linking basin-scale connectivity, oceanography and population dynamics for the conservation and management of marine ecosystems," Global Ecology and Biogeography **25**, 503–515 (2016).
[9] G. Froyland and M. Dellnitz, "Detecting and locating near-optimal almost-invariant sets and cycles," SIAM Journal on Scientific Computing **24**, 1839–1863 (2003).
[10] G. Froyland, "Statistically optimal almost-invariant sets," Physica D: Nonlinear Phenomena **200**, 205–219 (2005).
[11] G. Froyland, K. Padberg, M. H. England, and A. M. Treguier, "Detection of coherent oceanic structures via transfer operators," Physical Review Letters **98**, 224503 (2007).
[12] M. Dellnitz, G. Froyland, C. Horenkamp, K. Padberg-Gehle, and A. Sen Gupta, "Seasonal variability of the subpolar gyres in the Southern Ocean: a numerical investigation based on transfer operators," Nonlinear Processes in Geophysics **16**, 655–663 (2009).
[13] G. Froyland, N. Santitissadeekorn, and A. Monahan, "Transport in time-dependent dynamical systems: Finite-time coherent sets," Chaos: An Interdisciplinary Journal of Nonlinear Science **20**, 043116 (2010).
[14] N. Santitissadeekorn, G. Froyland, and A. Monahan, "Optimally coherent sets in geophysical flows: A transfer-operator approach to delimiting the stratospheric polar vortex," Physical Review E **82**, 056311 (2010).
[15] G. Froyland, C. Horenkamp, V. Rossi, N. Santitissadeekorn, and A. S. Gupta, "Three-dimensional characterization and tracking of an Agulhas Ring," Ocean Modelling **52**, 69–75 (2012).
[16] P. Tallapragada and S. D. Ross, "A set oriented definition of finite-time Lyapunov exponents and coherent sets," Communications in Nonlinear Science and Numerical Simulation **18**, 1106–1126 (2013).
[17] E. M. Bollt and N. Santitissadeekorn, *Applied and Computational Measurable Dynamics* (SIAM, Philadelphia, 2013).
[18] O. S. Galaktionov, P. D. Anderson, G. W. M. Peters, and H. E. H. Meijer, "Mapping approach for 3d laminar mixing simulations: application to industrial flows," International Journal for Numerical Methods in Fluids **40**, 345–351 (2002).
[19] M. K. Singh, P. D. Anderson, M. F. M. Speetjens, and H. E. H. Meijer, "Optimizing the rotated arc mixer," AIChE Journal **54**, 2809–2822 (2008).
[20] M. K. Singh, T. G. Kang, H. E. H. Meijer, and P. D. Anderson, "The mapping method as a toolbox to analyze, design, and optimize micromixers," Microfluidics and Nanofluidics **5**, 313–325 (2008).
[21] G. Froyland and M. Dellnitz, "Detecting and locating near-optimal almost-invariant sets and cycles," SIAM Journal on Sci-

entific Computing **24**, 1839–1863 (2003).
[22]M. Dellnitz, M. Hessel-von Molo, P. Metzner, R. Preis, and C. Schütte, "Graph algorithms for dynamical systems," in *Analysis, Modeling and Simulation of Multiscale Problems*, edited by A. Mielke (Springer Verlag, Heidelberg, 2006) pp. 619–645.
[23]N. Santitissadeekorn and E. Bollt, "Identifying stochastic basin hopping by partitioning with graph modularity," Physica D: Nonlinear Phenomena **231**, 95–107 (2007).
[24]M. E. J. Newman, *Networks: An Introduction.* (Oxford University Press, Oxford, 2010).
[25]N. Molkenthin, K. Rehfeld, N. Marwan, and J. Kurths, "Networks from flows-from dynamics to topology," Scientific Reports **4**, 4119 (2014).
[26]L. Tupikina, N. Molkenthin, C. López, E. Hernández-García, N. Marwan, and J. Kurths, "Correlation networks from flows. the case of forced and time-dependent advection-diffusion dynamics," PLoS ONE **11**, 1–12 (2016).
[27]N. Molkenthin, H. Kutza, L. Tupikina, N. Marwan, J. F. Donges, U. Feudel, J. Kurths, and R. Donner, "Edge anisotropy and the geometric perspective on flow networks," Chaos **This issue, to appear** (2017).
[28]A. Tsonis and P. Roebber, "The architecture of the climate network," Physica A: Statistical Mechanics and its Applications **333**, 497–504 (2004).
[29]K. Yamasaki, A. Gozolchiani, and S. Havlin, "Climate networks around the globe are significantly affected by El Niño," Physical Review Letters **100**, 228501 (2008).
[30]J. F. Donges, Y. Zou, N. Marwan, and J. Kurths, "Complex networks in climate dynamics," The European Physical Journal-Special Topics **174**, 157–179 (2009).
[31]M. Barreiro, A. C. Marti, and C. Masoller, "Inferring long memory processes in the climate network via ordinal pattern analysis," Chaos **21**, 013101 (2011).
[32]G. Froyland, K. Padberg, M. H. England, and A. M. Treguier, "Detection of coherent oceanic structures via transfer operators," Physical Review Letters **98**, 224503 (2007).
[33]G. Froyland, N. Santitissadeekorn, and A. Monahan, "Transport in time-dependent dynamical systems: Finite-time coherent sets," Chaos: An Interdisciplinary Journal of Nonlinear Science **20**, 043116 (2010).
[34]G. Froyland, R. M. Stuart, and E. van Sebille, "How well-connected is the surface of the global ocean?" Chaos: An Interdisciplinary Journal of Nonlinear Science **24**, 033126 (2014).
[35]P. Cvitanović, R. Artuso, R. Mainieri, G. Tanner, and G. Vattay, *Chaos: Classical and Quantum* (Niels Bohr Inst., Copenhagen, 2016).
[36]P. Holme and J. Saramäki, "Temporal networks," Physics Reports **519**, 97–125 (2012).
[37]M. Dellnitz, G. Froyland, C. Horenkamp, K. Padberg-Gehle, and A. Sen Gupta, "Seasonal variability of the subpolar gyres in the Southern Ocean: a numerical investigation based on transfer operators," Nonlinear Processes in Geophysics **16**, 655–663 (2009).
[38]G. Froyland, "An analytic framework for identifying finite-time coherent sets in time-dependent dynamical systems," Physica D: Nonlinear Phenomena **250**, 1–19 (2013).
[39]H. H. Lentz, T. Selhorst, and I. M. Sokolov, "Unfolding accessibility provides a macroscopic approach to temporal networks," Physical Review Letters **110**, 118701 (2013).
[40]M. E. J. Newman, "The structure and function of complex networks," SIAM Review **45**, 167 (2003).
[41]M. Newman, *Networks: An introduction* (Oxford University Press, 2009).
[42]J. Saramäki, M. Kivelä, J.-P. Onnela, K. Kaski, and J. Kertész, "Generalizations of the clustering coefficient to weighted complex networks," Phys. Rev. E **75**, 027105 (2007).
[43]G. Fagiolo, "Clustering in complex directed networks," Phys. Rev. E **76**, 026107 (2007).
[44]S. C. Shadden, F. Lekien, and J. E. Marsden, "Definition and properties of Lagrangian coherent structures from finite-time Lyapunov exponents in two-dimensional aperiodic flows," Physica D **212**, 271–304 (2005).
[45]M. Farazmand and G. Haller, "Computing Lagrangian coherent structures from their variational theory," Chaos: An Interdisciplinary Journal of Nonlinear Science **22**, 013128 (2012).
[46]E. N. Lorenz, "Deterministic nonperiodic flow." J. Atmos. Sci. **20**, 130–141 (1963).
[47]C. Sparrow, *The Lorenz Equations: Bifurcations, Chaos, and Strange Attractors*, Applied Mathematical Sciences 41 (Springer-Verlag, New York, 1982).
[48]D. Viswanath, "Symbolic dynamics and periodic orbits of the Lorenz attractor," Nonlinearity **16**, 1035 (2003).
[49]Z. Galias and W. Tucker, "Short periodic orbits for the Lorenz system," in *International Conference on Signals and Electronic Systems, 2008. ICSES '08* (2008) pp. 285–288.
[50]G. Madec, C. Bissery, E. Crochelet, B. Meola, C. Webster, J. Claudet, A. Chassanite, S. Marinesque, P. Robert, M. Goutx, C. Quod, P. Robert, M. Goutx, and C. Quod, "NEMO ocean engine." Tech. Rep. (Note du Pole de Modélisation, Institut Pierre-Simon Laplace (IPSL), 2008).
[51]P. Oddo, M. Adani, N. Pinardi, C. Fratianni, M. Tonani, D. Pettenuzzo, *et al.*, "A nested Atlantic-Mediterranean sea general circulation model for operational forecasting," Ocean Science **5**, 461 (2009).
[52]C. Millot and I. Taupier-Letage, "Circulation in the Mediterranean Sea," in *The Mediterranean Sea*, Handbook of Environmental Chemistry, Vol. 5K, edited by A. Saliot (Springer-Verlag, Berlin, Heidelberg, 2005) pp. 29–66.
[53]A. H. Nayfeh and B. Balachandran, *Applied Nonlinear Dynamics: Analytical, Computational and Experimental Methods* (John Wiley, New York, 1995).